

The Effect of Stepwise Postimplantation Annealing on the Composition and Structure of Silicon Surface Layers Implanted with Alkali Metal Ions

B. E. Umirzakov^{a*}, Z. A. Isakhanov^b, G. Kh. Allaerova^a, and R. M. Erkulov^b

^a Tashkent State Technical University, Tashkent, 100097 Uzbekistan

^b Institute of Ion Plasma and Laser Technologies, Academy of Sciences of Uzbekistan, Tashkent, 100125 Uzbekistan

*e-mail: be.umirzakov@gmail.com

Received August 3, 2020; revised September 17, 2020; accepted September 17, 2020

Abstract—The dynamics of changes in the crystal structure and in the elemental and chemical composition of Si surface layers implanted with Na⁺, Rb⁺, and Cs⁺ ions in the process of stepwise annealing under different temperature conditions has been studied. It is shown that, on the surface implanted with Na⁺ ions, a NaSi₂ film is formed after annealing it at a temperature of $T = 900$ K, a single-layer NaSi₂ coating is formed at $T = 1000$ K and the surface and near-surface Si layers are completely cleansed of the atoms of the alloying element, oxygen, and carbon at $T = 1100$ K.

Keywords: ion implantation, metal silicide, epitaxial layers, nanofilms, annealing, high-energy electron diffraction, single-layer coatings, ion dose.

DOI: 10.1134/S1063785021010120

Molecular and solid-phase epitaxy [1–6] and the method of low-energy ($E_0 \leq 5$ keV) ion implantation in combination with annealing [7–12] are widely used when creating nanosized two- and multilayer heterostructures that offer necessary combinations of materials for producing base components of modern nano-, micro-, and optoelectronics. Of these methods, only ion implantation allows one to obtain homogeneous continuous films with a thickness of $h \leq 40\text{--}50$ Å. The preparation of an atomically clean substrate surface and the prerequisite of high purity of the deposited (implanted) substances are the main requirements for obtaining such structures. All these processes are carried out under ultrahigh vacuum conditions ($P \leq 10^{-8}$ Pa). In cleaning single crystals of Si, it is very important to find a reliable way to minimize the presence of oxygen and carbon atoms on the surface. In [13], the optimal regimes of ion-plasma and chemothermal cleaning of the silicon surface were determined, which make it possible to reduce the concentration of C and O to zero (within the sensitivity of the Auger spectrometer at the level of about 0.1 at %).

Low-energy ions implanted at shallow depths create surface defects at the early stage of epitaxial film growth, which subsequently serve as crystal nucleation sites. The energy of ions stimulates the chemical reaction processes on the surface—in particular, the formation of thin transition layers [14–18]. Under certain conditions, ion bombardment promotes ion-stimu-

lated desorption of C and O atoms and other contaminants from the surface. However, there are still no reliable data on the results of studying the dynamics of changes in the morphology, composition, and structure of ion-implanted Si upon stepwise annealing in a wide temperature range.

This work is devoted to a study of changes in the composition and structure of the Si(111) surface layers implanted with alkali metal ions upon annealing under various temperature conditions.

Single-crystal *n*-type Si(111) samples with a diameter of 10 mm and a thickness of 0.5 mm were the subjects of study. Ion implantation, heating, and all analyses were carried out on the same experimental setup under a vacuum pressure of at least $P = 10^{-7}$ Pa. The energy of ions ranged from 1 to 5 keV, and their dose was $D \approx 10^{14}\text{--}10^{17}$ cm⁻². The ion sources were standard chloride salts of the corresponding alkaline elements with a purity of around 99.99 wt %. Before ion implantation, the ion sources were cleaned by prolonged heating. After cleaning the source, the concentration of O on the Si surface did not change during the formation of vapors of an alkaline element. To study the composition and structure, a set of methods, such as Auger electron spectroscopy (AES), high- and low-energy electron diffraction techniques (HEED and LEED, respectively), and secondary ion mass spectrometry (SIMS), were used: scanning electron microscope (SEM) images were obtained on a stan-

Table 1. Dependence of parameter a of different types of ions on their energy E_0

E_0 , eV	$a \times 10^{17}$, cm ²				
	Li ⁺	Na ⁺	K ⁺	Rb ⁺	Cs ⁺
500	6.0	6.8	21.3	36.5	49.0
600	5.5	6.54	20.1	38.8	50.2
700	5.6	6.8	20.2	43.2	53.1
800	6.8	8.18	26.2	44.2	54.5
900	8.9	9.8	30.1	43.8	57.6
1000	9.0	10.36	34.1	52.6	62.5
1100	7.08	9.27	35.6	53.5	62.0
1600	6.95	9.37	33.1	–	61.5

The dash sign indicates that there is no available measurement result.

dard ISM-6490 facility with a resolution of 5–6 nm, and HEED patterns were obtained on an EMR-2 device. The formation of a chemical bond between the atoms of the matrix and the implanted element was assessed by the change in the shape and position of the XVV Auger peaks, and the concentration of Si atoms, impurities and alloying elements was assessed by the change in the intensity of high-energy peaks. The atomic distribution depth profiles were determined by the AES method in combination with layer-by-layer etching with argon ions. For comparison, the structure of a Si surface with a single-layer MeSi_2 coating obtained by depositing Me on Si and subsequent annealing was investigated. After the formation of a single-layer MeSi_2 coating, work function φ_0 of the Si surface decreases to a minimum value. The work function of the surface was monitored using the contact potential difference method. The experimental technique is described in detail in [15].

During ion implantation, the surface layer becomes disordered and the atoms of the alloying element are introduced. The degree of surface disordering can be determined with high accuracy from LEED patterns. The change in the diffraction intensity will be determined from the combination of two effects: disturbance of the atomic arrangement and a change in the surface composition. To take into account the total effect, it is convenient to monitor the change in the surface defectiveness as a function of the ratio of the diffraction reflection intensities and the elastic background [15]. The reflection current and the background current are measured quantities that are proportional to the first powers of the areas occupied by the order and disorder, respectively. Therefore, the dependence of the ratio of the reflection current (I_r) to the background current (I_b) on the radiation dose has the following form, according to [15]:

$$I_r/I_b = (I_{r0}/I_{b0}) \exp(-aD),$$

where I_{r0}/I_{b0} the ratio of the reflection current to the background current before irradiation, a is the average area of disorder per one ion, and D is the radiation dose. Table 1 shows the experimental a values for different types of ions, which depend on their energy E_0 . It can be seen that the value of a varies nonmonotonically as a function of the ion energy (with a maximum at around 1000 eV and with a minimum at 650–700 eV). With an increase in the ion mass, the a value increases. At the same time, the a values measured from the degradation of merely the diffraction intensity can be compared, which were higher by more than 1.5 orders of magnitude.

Figure 1 shows the Auger spectra in the energy range of $E = 85$ – 100 eV (the $L_{23}VV$ Auger line of silicon) for pure Si and for Si samples implanted with Na^+ ions with $E_0 = 1$ keV at $D = 6 \times 10^{16}$ cm⁻² before and after annealing at $T \approx 900$ K for 30 min. As can be seen from Fig. 1, the intensity of the Si peak decreases sharply after ion implantation and new peaks characteristic of NaSi ($E = 96$ – 97 eV) and NaSi_2 ($E = 94$ – 95 eV) appear. After annealing at $T \approx 900$ K, the peaks corresponding to NaSi and Si disappear, while the peak of NaSi_2 increases to a maximum.

Figure 2 shows the dependences of the intensities of the Auger peaks of O (506 eV) and Na (992 eV) on depth d for well-purified Si(111) and for the same material after implantation with Na^+ ions with an energy of $E_0 = 1$ keV at $D = D_{\text{sat}} = 8 \times 10^{16}$ cm⁻², where D_{sat} is the saturation dose. The calculations performed on the basis of analyzing the Auger spectra showed that the concentration of O on the surface of pure Si is 1.5 at %. With an increase in d , the concentration of O decreases monotonically and barely changes starting from $d = 80$ – 100 Å, dwelling at a level of about 0.5 at % (curve 1 in Fig. 2). In the case of ion-implanted Si, oxygen atoms are practically not detected in the heavily doped region ($d \approx 0$ – 35 Å), but they accumulate in the region of a sharp decrease in the sodium content (curves 2, 3 in Fig. 2). Apparently, some part of the oxygen atoms evaporate from the surface during ion bombardment, while the other part diffuses deep into the sample to the ion-doped layer–silicon interface (curve 2 in Fig. 2). After annealing at $T \approx 900$ K, the surface concentration of Na is about 30–35 at % and the surface concentration of Si is about 65–70 at %, with all Na atoms forming a chemical bond with Si atoms. The concentration of these atoms barely change to a depth of 30–35 at %. Moreover, a NaSi_2 film with good stoichiometry is formed in these layers. In this case, there is no noticeable change in the distribution profile of O atoms. Annealing of this system at $T \approx 1000$ K leads to a decrease in the thickness of the NaSi_2 film to a monomolecular layer, and annealing at $T = 1100$ K leads to complete evaporation of Na atoms and its compounds with silicon and oxygen from the surface layers (within the sensitivity range of the Auger spectrometer). The SIMS results showed that the sur-

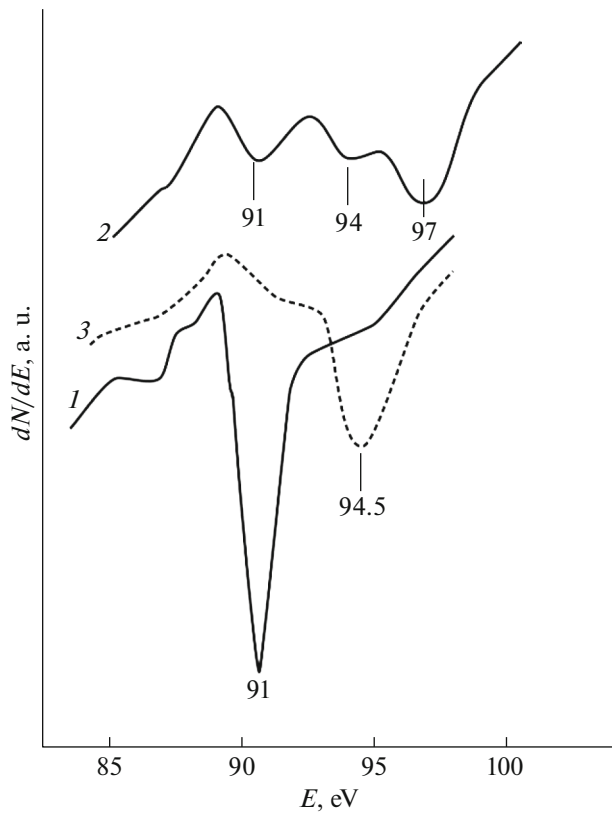


Fig. 1. Effects of implantation with Na⁺ ions and subsequent annealing on the intensity and position of the L₂₃VV Si Auger peak for (1) pure Si(111), (2) Si implanted with Na⁺ ions with E₀ = 1 keV at D = 8 × 10¹⁶ cm⁻², and (3) the sample after annealing of ion-implanted silicon at T = 900 K for 30 min. The Auger spectra were recorded at a primary electron energy of E_p = 2500 eV.

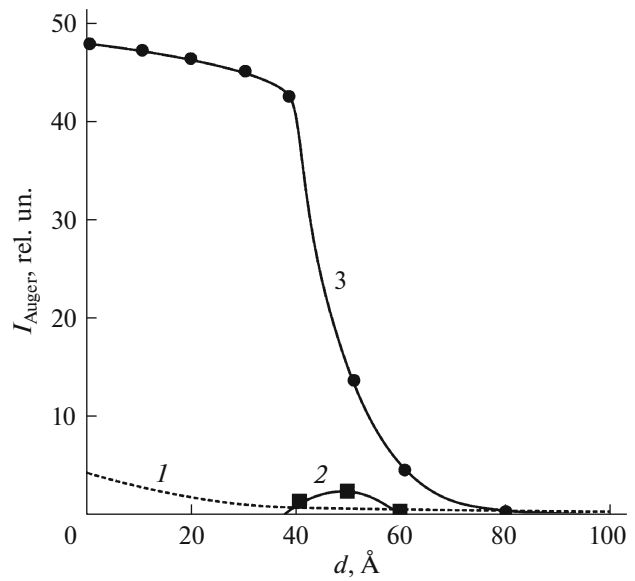


Fig. 2. Auger profiles of atomic depth distribution for (1) pure Si(111), (2) oxygen atoms in pure Si(111) implanted with Na⁺ ions with E₀ = 1 keV at D = 6 × 10¹⁶ cm⁻², and (3) sodium atoms in ion-doped silicon.

face and the near-surface region to a depth of 60–80 Å contain a very small amount of O in this case, the concentration of which does not exceed 0.1 at %, with the estimated values of the carbon concentration in these regions being about 0.02 at %. Just like in the case of unimplanted Si, the oxygen concentration at d ≥ 100–

150 Å remains almost unchanged and rests at a level of about 0.3–0.5 at %. Table 2 shows temperatures T_E of formation of epitaxial MeSi₂ layers, thickness h of these layers, temperatures T_M of formation of a monomolecular layer of silicide with relevant eφ_{min}, and temperatures T_{cr} required for complete cleaning of Si samples implanted with Na⁺, Rb⁺, and Cs⁺ ions with energies of 0.5 and 1.0 keV at D = D_{sat}. As can be seen from Table 2, the thickness of the MeSi₂ films formed at the same implantation energies in the case of Na⁺ is much larger than in the cases of Rb⁺ and Cs⁺. This is explained by the fact that the depth of penetration of alkaline element atoms at E₀ = const and the saturation dose increase with a decrease in their diameter and the temperature of formation of the silicide film

Table 2. Temperatures of formation of MeSi₂ silicide nanofilms, temperatures of formation of a monomolecular MeSi₂ layer, and temperatures of complete cleaning of the Si surface

Ion	E ₀ , keV	D, cm ⁻²	MeSi ₂ nanofilm		Monomolecular MeSi ₂ layer		T _{cr} , K
			T _E , K	h, Å	T _M , K	eφ, eV	
Na ⁺	0.5	6 × 10 ¹⁶	900	30–35	1000	2.1	1100
	1.0	8 × 10 ¹⁶	950	35–40	1000	2.1	
Rb ⁺	0.5	4 × 10 ¹⁶	850	–	950	1.95	1050
	1.0	6 × 10 ¹⁶	900	25–30	1000	2.0	
Cs ⁺	0.5	3 × 10 ¹⁶	700	–	800	1.8	900
	1.0	5 × 10 ¹⁶	700	20–25	–	–	

The dash signs indicate that no measurement results are available.

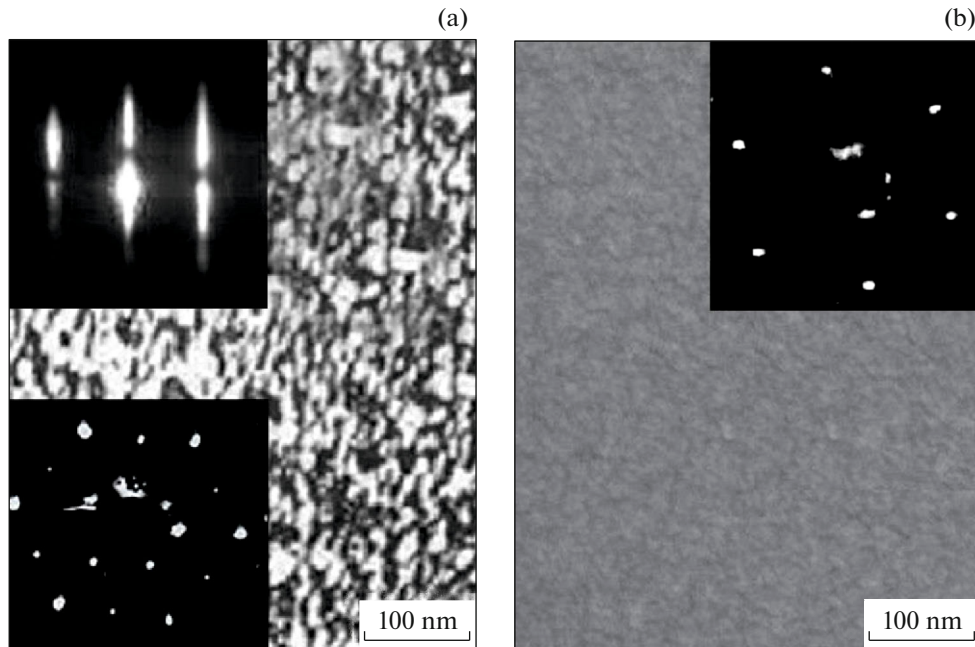


Fig. 3. (a) SEM image of the surface of the $\text{RbSi}_2/\text{Si}(111)$ film with a thickness of 35–40 Å. The upper inset shows the HEED pattern of the RbSi_2 film recorded with an electron beam energy of 15 keV, and the lower inset shows the LEED pattern of $\text{Si}(111)$ with a single-layer RbSi_2 coating; reflections with large diameters belong to Rb, and reflections with small diameters belong to mismatch defects. (b) The SEM image and LEED pattern (inset) of the surface of the $\text{RbSi}_2/\text{Si}(111)$ system obtained after annealing at $T = 1100$ K. The LEED patterns were obtained at $E_p = 54$ eV.

decreases. Critical temperature T_{cr} of surface cleaning and the thickness of the cleaned layers depends on the type and energy of the ions. For all alkali metal silicides, the temperature of complete surface cleaning is 1100 K. Such a high degree of purification could not be obtained by annealing unimplanted Si to $T \approx 1400$ –1500 K even in combination with ion etching. The high purity of the Si surface is preserved for 10–15 min under a vacuum of $P = 10^{-7}$ Pa and for 1.5–2 h in a vacuum of $P = 10^{-9}$ Pa.

Figure 3a shows an SEM image and an HEED pattern (upper inset) for the RbSi_2 film obtained after annealing at $T = 900$ K on the silicon surface implanted with Rb^+ ions with $E_0 = 1$ keV at a dose of $D = 6 \times 10^{16}$ cm^{-2} . Figure 3a also shows the LEED pattern (lower inset) obtained after heating this system at $T = 1000$ K. As can be seen from Fig. 3a, the surface of the RbSi_2 film is relatively smooth and the film grew epitaxially (upper inset), while the Si surface with a single-layer RbSi_2 coating has a 2×2 structure (lower inset). The latter completely coincides with the 2×2 RbSi_2 structure obtained in our earlier study [15] by low-temperature deposition of layers from ion beams with a low energy ($E_0 \approx 500$ eV) and a low dose ($D \approx 10^5$ cm^{-2}). Our further studies showed that all silicides of alkali metals of the MeSi_2 type grow epitaxially; nevertheless, their surface has different structures. For

example, the surface of a single-layer LiSi_2 coating has a 3×3 structure, while NiSi_2 has a 1×1 structure.

Regardless of the type of silicide film, its complete evaporation and the evaporation of oxygen and carbon atoms are observed after annealing at $T = 1100$ K. The Si surface becomes homogeneous and smooth (Fig. 3b), and the 1×1 structure characteristic of pure silicon is restored (Fig. 3b, inset).

Thus, the dynamics of changes in the composition and structure of the surface layers of ion-implanted silicon upon annealing under different temperature conditions was studied for the first time. It is shown that the following changes occur at different temperatures: complete crystallization of ion-doped Si layers and the formation of silicides of the MeSi_2 type, the formation of a single-layer MeSi_2 coating, and maximum purification of the surface and near-surface Si layers.

CONFLICT OF INTEREST

The authors declare that they have no conflict of interest.

REFERENCES

1. L. Chang and K. Ploog, *Molecular Beam Epitaxy and Heterostructures* (Springer, Netherlands, 1985).

2. V. V. Zolotarev, A. Yu. Leshko, A. V. Lyutetskii, D. N. Nikolaev, N. A. Pikhtin, A. A. Podoskin, S. O. Slipchenko, Z. N. Sokolova, V. V. Shamakhov, I. N. Arsent'ev, L. S. Vavilova, K. V. Bakhvalov, and I. S. Tarasov, *Semiconductors* **47**, 122 (2013). <http://journals.ioffe.ru/articles/4885>.
3. M. A. Putyato, N. A. Valisheva, M. O. Petrushkov, V. V. Preobrazhenskii, B. R. Semyagin, E. A. Emel'yanov, A. V. Vasev, A. F. Skochkov, G. I. Yurko, and I. I. Neshterenko, *Tech. Phys.* **64**, 1010 (2019). <https://doi.org/10.1134/S106378421907020X>
4. M. A. Green, K. Emery, Y. Hishikawa, W. Warta, E. D. Dunlop, D. H. Levi, and A. W. Y. Ho-Baillie, *Prog. Photovolt.: Res. Appl.* **25**, 3 (2017). <https://doi.org/10.1002/pip.2855>
5. P. R. C. Kent and A. Zunger, *Phys. Rev. B* **64**, 115208 (2001). <https://doi.org/10.1103/PhysRevB.64.115208>
6. V. I. Rudakov, Yu. I. Denisenko, V. V. Naumov, and S. G. Simakin, *Tech. Phys. Lett.* **37**, 112 (2011). <http://journals.ioffe.ru/articles/12465>.
7. S. B. Donaev, F. Djurabekova, D. A. Tashmukhamedova, and B. E. Umirzakov, *Phys. Status Solidi C* **12**, 89 (2015). <https://doi.org/10.1002/pssc.201400156>
8. B. E. Umirzakov, T. S. Pugacheva, A. T. Tashatov, and D. A. Tashmukhamedova, *Nucl. Instrum. Methods Phys. Res., Sect. B* **166–167**, 572 (2000). [https://doi.org/10.1016/S0168-583X\(99\)01151-9](https://doi.org/10.1016/S0168-583X(99)01151-9)
9. Z. A. Isakhanov, Z. E. Mukhtarov, B. E. Umirzakov, and M. K. Ruzibaeva, *Tech. Phys.* **56**, 546 (2011). <https://doi.org/10.1134/S1063784211040177>
10. Y. S. Ergashov, B. E. Umirzakov, and G. Kh. Allayarova, *Mater. Sci. Appl.* **9**, 965 (2018). <https://doi.org/10.4236/msa.2018.912069>
11. Kh. Kh. Boltaev, D. A. Tashmukhamedova, and B. E. Umirzakov, *J. Surf. Invest.: X-ray, Synchrotron Neutron Tech.* **8**, 326 (2014). <https://doi.org/10.1134/S1027451014010108>
12. S. B. Donaev, *Tech. Phys. Lett.* **46**, 796 (2020). <https://doi.org/10.1134/S1063785020080192>
13. A. G. Ozerov, A. A. Altukhov, V. V. Ivanov, and E. A. Titova, *Tekh. Sredstva Svyazi, Ser. TPO, No. 1*, 111 (1987).
14. L. Pelaz, L. A. Marques, and J. Barbolla, *J. Appl. Phys.* **96**, 5947 (2004). <https://doi.org/10.1063/1.1808484>
15. B. E. Umirzakov, S. Zh. Nimatov, and D. S. Rumi, *Structure and Properties of Multilayer Nanofilm Systems Based on Silicon* (Infinity Group, Tashkent, 2013) [in Russian].
16. J. Matsuo, T. Aoki, and T. Seki, in *Proceedings of the 2007 International Workshop on Junction Technology* (Kyoto, 2007), p. 53. <https://doi.org/10.1109/iwjt.2007.4279945>
17. S. Zh. Nimatov, B. E. Umirzakov, F. Ya. Khudaikulov, and D. S. Rumi, *Tech. Phys.* **64**, 1527 (2019). <https://doi.org/10.1134/S1063784219100153>
18. B. E. Umirzakov, D. A. Tashmukhamedova, G. Kh. Allayarova, and Zh. Sh. Sodikzhanov, *Tech. Phys. Lett.* **45**, 356 (2019). <https://doi.org/10.1134/S1063785019040175>

Translated by O. Kadkin